

# 15. Department of Engineering and Technical Services

The Department of Engineering and Technical Services covers a wide range of work in the design, fabrication, construction, and operation of experimental devices in the fields of software and hardware.

The department consists of the following five divisions. The Fabrication Technology Division oversees the construction of small devices and the quality control of parts for all divisions. The Device Technology Division works on the Large Helical Device (LHD) and its peripheral devices except for heating devices and diagnostic devices. The Plasma Heating Technology Division supports the ECH system, the ICRF system, and the NBI system. The Diagnostic Technology Division supports plasma diagnostic devices and radiation measurement devices, and oversees radiation control. Finally, the Control Technology Division concentrates on the central control system, the cryogenic system, the current control system, and the NIFS network.

The total number of staff is now 59 (2020). We have carried out the development, the operation, and the maintenance of the LHD and those peripheral devices together with approximately 57 operators.

(S. Kobayashi)

## 1. Fabrication Technology Division

The main work of this division is the fabrication of experimental equipment. We also take care of technical consultation and experimental parts supplies related to the LHD experiment. In addition, we manage the administrative procedures of the department.

The number of machined requests was 127, and the production parts total number was 533 in this fiscal year (FY). The total numbers of electronic engineering requests and articles were 16 and 45, respectively. The details of some of this division's activities follow below.

(M. Yokota)

### (1) Fabrication of Corrugated Conductor

A cylindrical cavity wall with periodical corrugation to excite a cylindrical Bloch wave at the frequency of 100 GHz was fabricated as shown in Fig. 1.

The cylindrical conductor has 80 corrugations on the outside. The parameters of the rectangular corrugation are a width of 0.3 mm, a depth of 0.6 mm, and a periodic length of 0.5 mm.

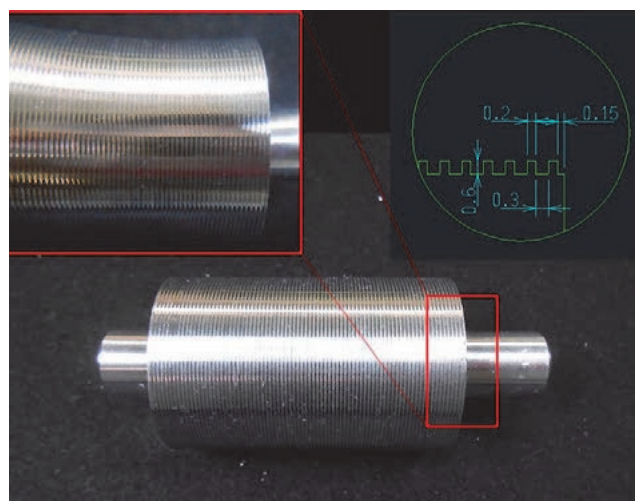


Fig. 1 Corrugated Conductor.

(K. Okada)

(2) Fabrication of 56 GHz notch filter

A 56 GHz Notch filter was fabricated for the Electron Cyclotron Emission Imaging System(Fig. 2). It consists of 6 cavities and a waveguide in the internal space.

The parameters of the cavity analyzed for electromagnetic fields are a diameter of 4.12 mm, and a depth of 4.63 mm. And the parameters of the rectangular waveguide are a length of 5.69 mm, and a width of 2.845 mm.

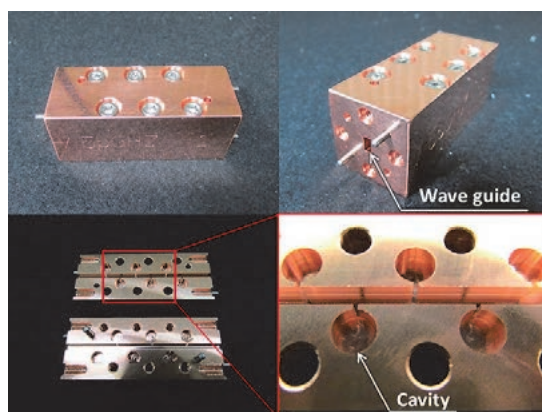


Fig. 2 56 GHz notch filter.

(T. Shimizu)

(3) Fabrication of 35ch PN photo diode array amplifier

A 35ch PN photo diode array amplifier is used to amplify the emission spectral signal when the solid hydrogen pellets melt in the plasma (Fig. 3).

This circuit has the specifications that the frequency bandwidth is DC to 2 MHz, and the current-voltage conversion resistance is 1 M $\Omega$ .

A problem of mutual interference, because the amplifiers were densely packed around the PN element, was solved by a noise reduction effect using a guard electrode for the signal line.

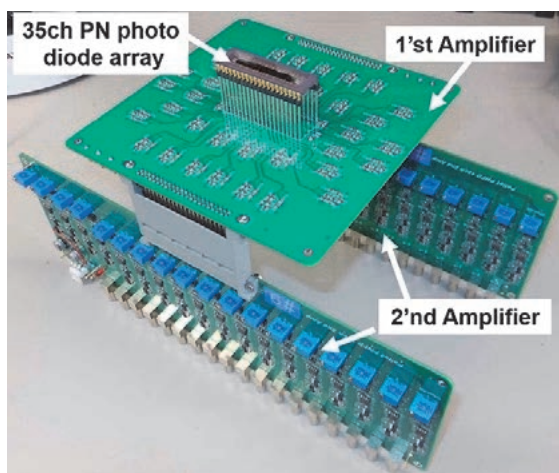


Fig. 3 35ch PN photo diode array amplifier.

(Y. Ito)

## 2. Device Technology Division

This Division supports the operation, improvement, and maintenance of LHD.

### (1) LHD operation

We started pumping the cryostat vessel for cryogenic components on August 27, 2020 and pumping the plasma vacuum vessel on August 28, 2020. Subsequently, we checked for air leakage from the flanges on the plasma vacuum vessel. Fifty-nine flanges were inspected. Consequently, we observed leakage in one device and repaired the device.

The pressure of the cryostat vessel reached the adiabatic condition ( $< 2 \times 10^{-2}$  Pa) on August 28, 2020, and the pressure of the plasma vacuum vessel was below  $1 \times 10^{-5}$  Pa on September 7, 2020.

The LHD experiments of the 22nd LHD experimental campaign were started on October 15, 2020, and carried out until February 18, 2021. The total number of days of the plasma experiments was 60.

During this experimental campaign, the vacuum pumping system eliminated air from both vessels without difficulty. In addition, no significant problems were reported for the utilities (for example, compressed air system, water-cooling system, GN2-supply system) of the LHD and the exhaust detritiation system. The LHD operation was completed on March 12, 2021.

(H. Hayashi)

### (2) Development of bonding technique with W and Cu alloys using an advanced spark plasma sintering method

A bonding technique was developed using a tungsten (W) and copper (Cu) alloy, with chromium zirconium copper (CuCrZr) as a divertor material in the LHD. The two materials were bonded using the powder solid bonding (PSB) method, as shown in Fig. 4, an advanced spark plasma sintering method. Based on this method, a hydrogen environment was prepared, where the bonding process was performed to suppress the oxidation of W effectively, which would otherwise reduce the bonding strength of the materials. Furthermore, a mixed powder of W and Cu was inserted between W and CuCrZr to minimize the thermal stress generated at the bonded interface owing to the difference in the thermal expansion coefficients between W and CuCrZr. Shear strength tests were performed on the test specimens to evaluate the quality and strength of the bonding between the two materials, and the bond strength at the bonded interface was measured. The quality of the bonded interface was further verified through electron microscopy, qualitative and quantitative analysis, elemental mapping images, hardness measurements, and ultrasonic testing. The results showed that the intermediate layer of the W–Cu mixed powder was sufficiently dense, and no undesirable defects appeared on the intermediate layer or at the bonded interface. The proposed method will help manufacture more reliable and effective heterometallic bonding materials without defects in fusion experimental devices.



Fig. 4 Bonding samples fabricated using PSB method.

(T. Murase)

### (3) Development of water bubbler system for tritium measurements in gas flow

When a deuterium (D) plasma experiment is conducted, tritium is generated through the D-D fusion reaction, and then a part of the tritium is implanted in the plasma-facing materials (PFMs). A water bubbler system was

designed and constructed as equipment for the tritium analysis system to evaluate the amount of tritium in the PFMs. A flow diagram of the water bubbler system is shown in Fig. 5.

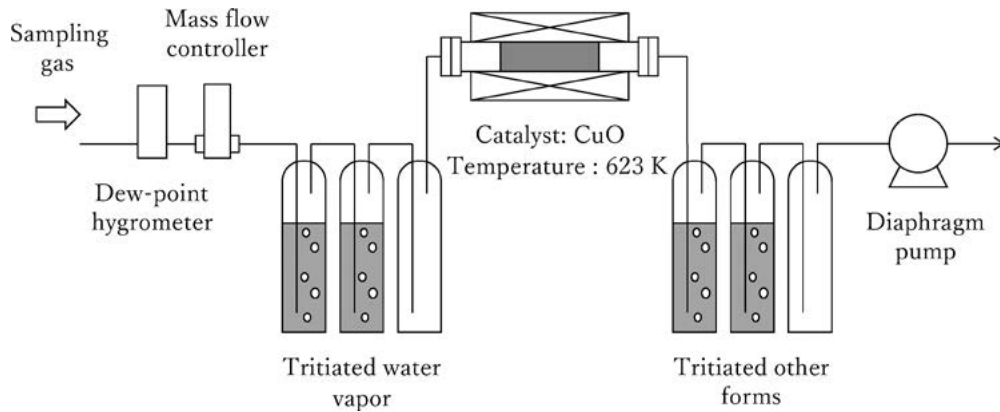


Fig. 5 A flow diagram of the water bubbler system.

The water bubbler system can collect tritium in water, and the chemical forms of tritium, such as water vapor and other chemical forms, are discriminated by a catalytic reactor packed with copper oxide (CuO wire approximately  $0.65 \times 6$  mm, PN: 1.02767, Millipore Corporation). The catalytic heater can be heated to 723 K. This system is controlled using a programmable logic controller that incorporates the settings of the sampling time or temperature control and, the interlock of the catalytic heater.

After the sampling operation, the water sample containing tritium was mixed with a liquid scintillator (Ultimate Gold LLT, PerkinElmer) in a polyethylene vial. Then mixed sample was measured using a liquid scintillation counter (Tri-Carb 4910TR, PerkinElmer).

The performance of the developed system was compared with that of a conventional system. The results showed a good agreement, as summarized in Table 1.

Table 1 Measurement results

Devices	Run1 (Bq/cm <sup>3</sup> )	Run2 (Bq/cm <sup>3</sup> )
Conventional system	$10.7 \times 10^{-5} \pm 9.4 \times 10^{-6}$	$7.9 \times 10^{-5} \pm 7.5 \times 10^{-6}$
Developed system	$8.1 \times 10^{-5} \pm 7.0 \times 10^{-6}$	$7.9 \times 10^{-5} \pm 7.4 \times 10^{-6}$

(H. Kato)

#### (4) Development of a new ion source for heavy ion beam probes

The plasma potential is a critical parameter in plasma research, and it has been measured using heavy ion beam probes (HIBP).

Currently, the problem of HIBP is that it is difficult to measure the plasma potential in high-density regions. It is necessary to develop a new ion source as shown in Fig. 6 to increase the ion beam current. The target beam current is 100  $\mu$ A, which is five times higher than the current ion beam current.

In the current ion source, argon is ionized using a heater and sputtered onto gold to produce negative gold ions. In the new ion source, the heater is bowl-shaped, and it ionizes cesium and collects it at one point, similar to a lens. This process efficiently spatters the cesium onto gold to produce negative gold ions.

In developing the new ion source, five power supplies, including a heater power supply for cesium vaporization, a beam current measurement device, and a device for cooling the equipment, were selected, purchased, and installed. Additionally safety measures were implemented.

The performance test of the new ion source showed that the beam current was only 28  $\mu\text{A}$  at the center of the beam. The new ion source is integrated into the HIBP system of the LHD after adjustment to improve beam focusing.

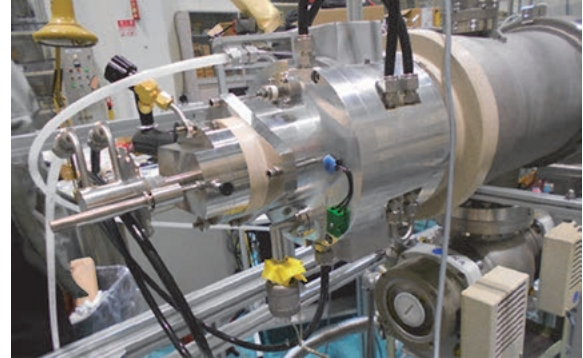


Fig. 6 New ion source for the HIBP.

(H. Takubo)

### (5) Development of scroll pump load current monitoring system

We built a load current monitoring system for scroll pumps. This action was performed to check for a pump failure rapidly. We monitored the load current of the scroll pump during operation and determined the state of the pump.

We installed one Rogowski coil clamp on each pump and recorded the condition of the pumps. We stopped running the pump because we observed an increase in current, signifying the failure of the pump as shown in Fig. 7. Consequently, the pump damage was minimized. We believe that the proposed system is effective for preventing pump damage.

In the future, we will expand the scope of this system and strengthen the management of pumps.



Fig. 7 Increased load current.

(H. Chimura)

## 3. Plasma Heating Technology Division

The main tasks of this division are the operation and the maintenance of three different types of plasma heating devices and their common facilities. We have also performed technical support for improving, developing and

newly installing these devices. In this fiscal year, we mainly carried out device improvement and modification for a deuterium plasma experiment. The details of these activities are as follows.

(T. Kondo)

(1) ECH

(a) Gyrotron Operation for LHD experiments and Developments of devices

During the 22nd experimental campaign, we injected power up to 4 MW to assist plasma experiments. That contributed to the accomplishment of high performance plasmas with high ion and electron temperatures. Low power and long pulse injection can sustain the ECH plasma. Some trouble happened, but all ECH technical staff of the LHD experimental group contributed to the various plasma experiments.

The gyrotron have three kinds of high-voltage power supply (Anode, Body, and Collector). We designed the high-voltage switch device, which can connect or disconnect three power supplies in simultaneously by a pneumatic actuator (Fig. 8).

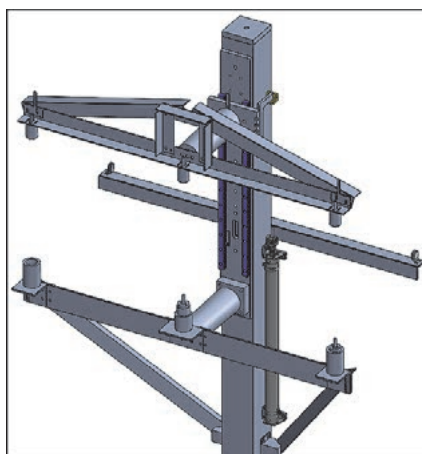


Fig. 8 A picture of the high-voltage switch device.

(S. Ito and T. Takeuchi)

(2) ICH

(a) The operation of ICH in the 22nd experimental campaign of LHD experiments

In the 22nd experimental campaign, HAS (Handshake type) antennas with two antenna straps were installed at the 3.5U&L ports of the LHD. Thus, in addition to the FAIT (Field-Aligned Impedance-Transforming) antenna with two antenna straps at the 4.5U&L ports, we carried out the LHD experiments with in total two antennas with four antenna straps.

We decided the combination of an RF transmitter and an antenna strap. Then, the transmitters #3 and #4 were connected to the 3.5U&L antenna straps and transmitters #6A and #6B were connected to the 4.5U&L antenna straps. The total injection power from the four antenna straps into the plasma reached about 3.4 MW in the short pulse of 1 second at the RF wave frequency of 38.47 MHz.

(b) Development of high-speed optical measurement system “Ha-fast”

We developed an optical measurement system to detect the passive emissions of  $H\alpha$  (656.3 nm), HeI

(587.6 nm), and HeII (468.6 nm) with time resolution higher than 1 MS/s. These data are registered with LABCOM as the diagnostic name “Ha-fast”. Fig. 9 shows a diagram of this system, and Fig. 10 shows a measurement example. This system has observed the optical emissions of the ICH plasma successfully.

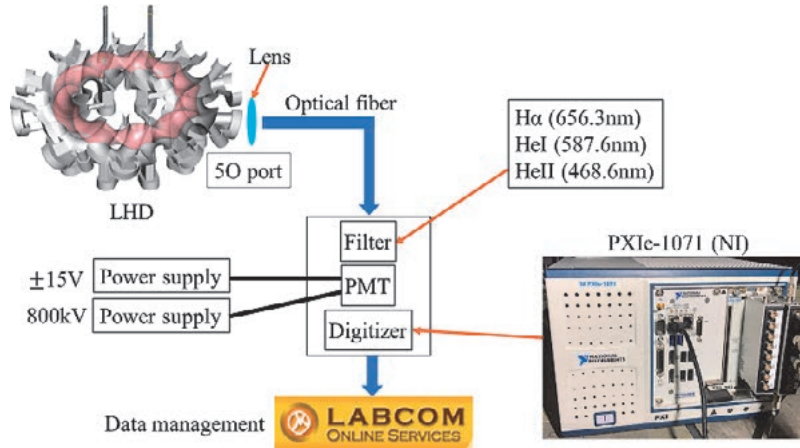


Fig. 9 A diagram of an optical measurement system.

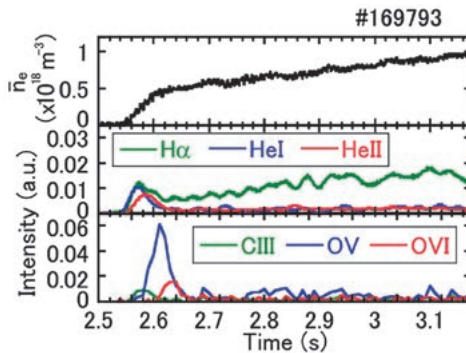


Fig. 10 A measurement example.

(G. Nomura and M. Kanda)

(3) NBI

(a) The operation and maintenance of NBI in the 22nd campaign of LHD experiments

In this campaign, approximately 8,000 shots of beams were injected into the LHD plasmas with three negative-NBIs (BL1, BL2, and BL3). The injection history of the total injection power for the negative-NBIs is shown in Fig. 11. The maximum injection power in this campaign was about 12MW. As for the positive-NBIs (BL4 and BL5), the maximum total injection power of the positive-NBIs was about 20MW. The NBIs had no troubles that lead to serious problems in the plasma experiments.

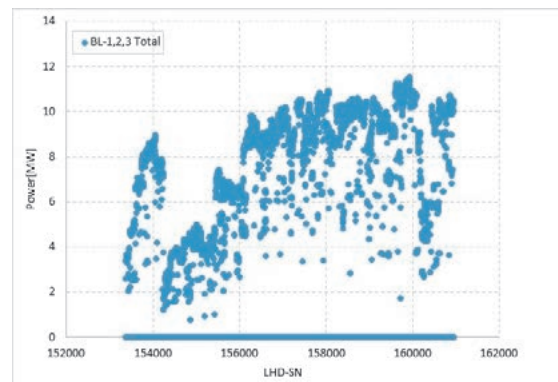


Fig. 11 A history of the total injection power for the negative-NBIs.

**(b) Evaluation of NBI injection power**

NBI injection power is evaluated from the temperature rise of Calorie-Meter Arrays (CMA), which consist of molybdenum chips and are installed in armor tiles at the wall opposite to the NBI injection-port. The temperatures of calorie-meter chips are measured by sheath type thermocouples via isolation amplifiers using a WE (YOKOGAWA Co.) data acquisition system. Under the weak magnetic field configuration of LHD, energetic particles from plasmas often hit some of molybdenum chips of the CMA. In this case, the temperatures of these chips are not used in the evaluation.

The NBI injection efficiency is estimated by normalizing the evaluated NBI injection power by the output power of the acceleration power supplies. Here, the monitor signals of the power-supply outputs are acquired by the CAMAC data acquisition system. The typical estimated injection efficiencies for three tangential NBIs, are shown for the 22nd campaign of LHD experiments, as follows.

NBI1: 0.333(H), 0.334(D)

NBI2: 0.256(H), 0.226(D)

NBI3: 0.325(H), 0.275(D)

(M. Sato and S. Komada)

**(4) Motor-Generator (MG)**

The MG is used to supply the pulsed power to the NBI and the ECH for LHD. The MG has supplied power for 20,740 shots in this fiscal year and 674,473 shots since its construction. The operation time was 1,208 hours. 136 batteries have been replaced for control and braking.

(Y. Mizuno)

**4. Diagnostics Technology Division**

This division mainly supports the development, the operation and the maintenance of plasma diagnostic devices and radiation measurement devices for LHD. In addition, we also have taken charge of radiation control.

(T. Kobuchi)

**(1) Plasma diagnostic device**

Some plasma diagnostics devices have functioned for more than 20 years and thus require maintenance.

For the Nd:YAG Thomson scattering system, we replaced a noise cut transformer and outlets for the data acquisition system power supplies with new ones (Fig. 12). As a result of them, fast bus error incidence decreased by about 40% in the data acquisition system from the previous experimental campaign.

For the FIR interferometer (far-infrared laser measuring device), we have updated from the recording device using an analog chart paper and a pen to the magnetic recording device as shown in Fig. 13. It became possible to collect the data in more detail, to read the data from memory and to create graphs, when necessary.

For the integrated radiation monitoring system, we are developing the programs to operate some equipment. The program which reads personal data from an ID card has been developed for identifying the person who is operating.

The LHD data acquisition system began acquiring images from 15 surveillance camera measurements in the 22nd experimental campaign and acquired a total data volume of approximately 312.7 TB in compressed size. This is more than three times the amount of data collected in the 21st experimental campaign, so both RAID storage and optical disk storage were suddenly expanded to store a large amount of data during the experiment.



Fig. 12 Outlets for data acquisition system power supplies in the Thomson scattering system.

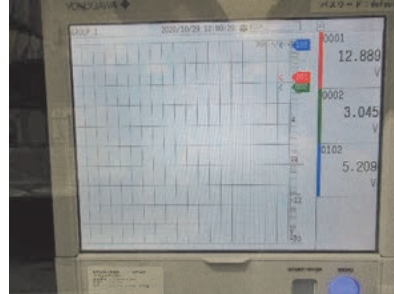


Fig. 13 Display of the new recording device.

(C. Iwai, T. Nishimura and M. Ohsuna)

(2) Radiation measurement and radiation control

In order to control the safety of radioactivity, we carried out the operation and maintenance of three high-purity germanium (HPGe) detectors, seven liquid scintillation counters, a  $2\pi$  gas-flow counter, an auto well gamma system, three stack tritium monitoring systems, two gas monitoring systems, two dust monitoring systems, and the drain water monitoring system. The liquid scintillation counters are used for exhaled tritium measurement, exhaust tritium measurement, wastewater measurement, and environmental water measurement.

In the application system for radiation worker registration, the SQRC for access control to be pasted on the Luxcel badge had been printed by receiving the EXCEL list, converting it to CSV, and using a special application, but a program was developed to allow direct printing from the WWW browser to improve the efficiency of the work (Fig. 14).

We are developing the program to operate some equipment connected to the integrated radiation monitoring system. The program which reads personal data from an ID card has been developed for identifying the person who operates the equipment.



Fig. 14 Pressing the button indicated by the red circle will start printing the SQRC (in Japanese).

(M. Nakada, S. Hashimoto, M. Nonomura and Y. Yamamoto)

5. Control Technology Division

The Control Technology Division is in charge of the important engineering tasks in the LHD project, such as system development, project management and system operation, which are mainly targeted to the central control

system, cryogenic system, coil power supply and super-conducting coils.

We are also responsible for the IT infrastructures, e.g. LHD experiment network, NIFS campus information network and internet servers, in every phase of the projects including requirements analysis, system design, implementation, operation and user support.

The essential topics of the activities for last fiscal year are described below.

(H. Ogawa)

### (1) LHD cryogenic system and power supply system for superconducting coils

The cooling operation in the 22nd experimental campaign has been executed without significant accident.

In the power supply system, we replaced the monitoring and logging devices for coil energization before the 21st experimental campaign. This fiscal year we have developed the waveform display application for the long-time data monitoring and logging using LabVIEW (Fig. 15) because the application originally attached to the device had a limited display time of up to 1 second.

Major functions are as follows: 1) 48 simultaneous monitoring channels, 2) automatic logging start/stop, 3) variable length of data display time up to 2 hours and 4) device status monitoring.

The new application monitored and recorded all signals with no severe problems in the 22nd experimental campaign.



Fig. 15 Newly developed waveform display application.

(H. Tanoue)

### (2) Development of current Timing Modulator

In the LHD plasma experiment, the current Timing Modulator, which provides timing signals to the measurement equipment, has been used for over 20 years since the 1st experimental campaign. Therefore, we developed the replacement modulator in case of an unpredictable failure caused by deterioration.

Once the modulator receives a pulse signal from the Central Control System, it sends modulated signals to

the demodulators. Then, the demodulators control measurement equipment according to the signal type they have received.

The new modulator adopts a FPGA board with a Zynq processor called Microzed, manufactured by Xilinx Inc., and the same functions as the current modulator are implemented using development tools, Vivado and PetaLinux (Fig. 16).

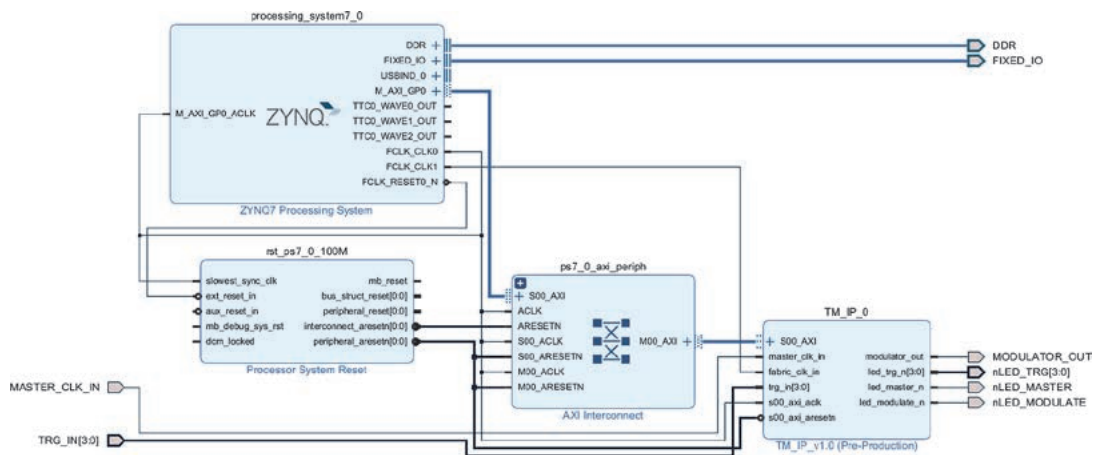


Fig. 16 Block design of the timing modulator.

(H. Maeno)

(3) Network management

The NIFS campus information networks consist of several clusters. We manage the Research Information Cluster (NIFS-LAN) and the LHD Experiment Cluster (LHD-LAN).

The achievements in FY 2020 are as follows:

(a) Introduction of G suite for Education

Along with the introduction of G suite for Education, a cloud service provided by Google, the mail system was migrated from an on-premise mail server system to Gmail.

(b) Upgrade of the virtual server system

The virtual server system has been upgraded (Fig. 17). Although the number of servers was reduced from four to three, the number of virtual machines that could be installed to the server increased due to the upgrade of the CPU, memory size and the other resources.

(c) LHD-LAN

It is required in our security policy that the network management staff needs to be present when connecting a new device to the LHD-LAN.



Fig. 17 Virtual server system.

In FY 2020, the 66 new devices were connected to the LHD-LAN, 88 were updated and 26 IP addresses made available due to device removal.

(T. Inoue and O. Nakamura)

### 6. Development of a double-barreled Tracer-Encapsulated Solid Pellet (TESPEL) injection system (TESPEL#4)

We have developed and installed a TESPEL#4 system, which will be one of the important experimental tools for the LHD. We have already made two TESPEL injection systems (one for the LHD, and the other for the German magnetic fusion experiment device, Wendelstein 7-X). Therefore, we have enough knowledge and technique for developing a new TESPEL injector. Thus, we accepted a request from a researcher to make the TESPEL#4 for the LHD. The significant features of the TESPEL#4 are that 1) it is a double-barreled system, and then it is possible to inject two TESPELs almost simultaneously, 2) the exchange cycle of the TESPEL holding disk can be reduced.

A compact design is necessary due to the limited available space for the TESPEL#4. For ensuring the performance of the TESPEL#4 system, we spent a lot of time on TESPEL injection tests and He leak tests. Fig. 18 shows a TESPEL#4 installed on the LHD. We developed the TESPEL#4 operation control system using a PLC. We also developed the remote control system for the TESPEL#4 operation with Microsoft Visual Studio. Fig. 19 shows an operation screen of the remote control system for the TESPEL#4. Fig. 20 shows the PLC and controllers

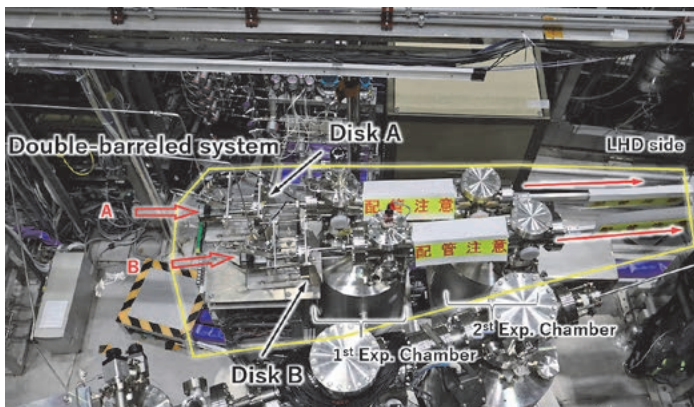


Fig. 18 TESPEL#4 installed on the LHD.

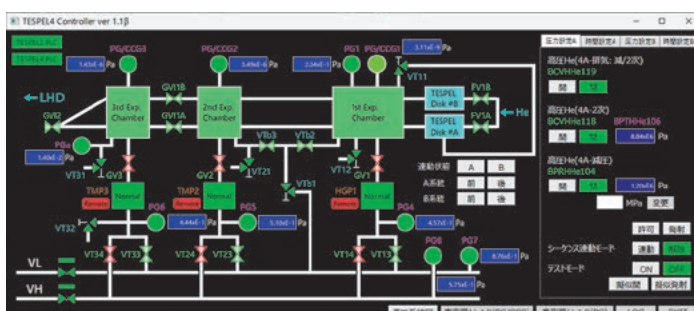


Fig. 19 Operation screen of remote control system for the TESPEL#4.



Fig. 20 PLC and controllers of the TESPEL#4.

of the TESPEL#4. The development of the TESPEL#4 system by the NIFS Engineering Department could keep development costs down., and it also can provide fast troubleshooting. In the 22nd LHD experiment campaign, we confirmed a successful injection of two TESPELs into a single discharge with the TESPEL#4 system.

(Hiromi Hayashi, H. Maeno and H. Furuta)

## 7. NIFS Article Information System (NAIS)

A list of rehearsal materials for the conference was made available on the NAIS so that we can check the materials to be presented online. As a result, we no longer need to post the materials, so we do not need to print them and can check them on our own PC (Fig. 21).



Fig. 21 The person in charge of the meeting can choose to make materials open or closed.

(M. Nonomura)

## 8. Activities of technical exchange and technical cooperation

### (1) Fourth technical exchange meeting: “Computational technology using finite element method”

On February 25, 2021, we held a technical exchange meeting on numerical computational technology based on the finite element method (FEM). This meeting was the fourth, and there were seven presenters and 40 participants, including those who used a remote web conference application (ZOOM), as shown in Fig. 22.

In this meeting, four outside presenters presented reports on reduced-order modeling technology using a commercial FEM code (ANSYS), the heat-transfer analysis of beam dumps and an accelerator production target using ANSYS Mechanical, the electromagnetic (EM)-force analysis of a port plug for JT60SA using ANSYS Emag, and the EM and structural analyses of toroidal-field magnetic coils on a reversed field pinch device, RELAX. In addition, three presenters within NIFS presented EM shield performance evaluation by comparing



Fig. 22 Technical exchange meeting using ZOOM meeting system.

the experimental and FEM results using ANSYS Maxwell, the modal and structural analyses of control cabinets required for experimental fusion devices, and the EM analysis and fabrication of a microwave notch filter using ANSYS HFSS. We engaged in discussions related to all the presentations.

(T. Murase)

(2) Fabrication of a model of the plasma experimental device “RT-1”

A model of the plasma experimental device “RT-1” was fabricated using a 3D printer at the request of the University of Tokyo as a technical cooperation.

This is a 1/30 size model, we delivered two units in a case with a two-color printed base (Fig. 23).

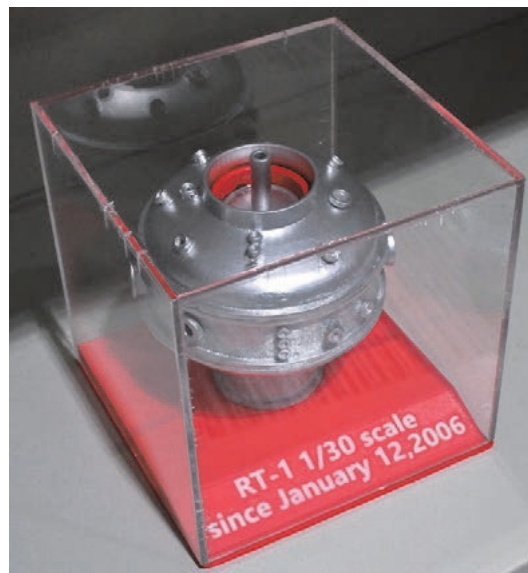


Fig. 23 1/30 size model of “RT-1”.

(S. Nakagawa and Y. Yamamoto)